frontiers in Earth Science

ORIGINAL RESEARCH
published: 24 March 2021
doi: 10.3389/feart.2021.578437

Low-Energy Fragmentation Dynamics at Copahue Volcano (Argentina) as Revealed by an Infrasonic Array and Ash Characteristics

Marcia Hantusch[1,2], Giorgio Lacanna[3], Maurizio Ripepe[3], Veronica Montenegro[1,2], Oscar Valderrama[4], Camila Farias[5], Alberto Caselli[1,2], Pietro Gabellini[3] and Raffaello Cioni[3]*

[1]Instituto de Investigación en Paleobiología y Geología, Universidad Nacional de Río Negro, General Roca, Argentina, [2]Consejo Nacional de Investigaciones Científicas y Técnicas (CONICET), Buenos Aires, Argentina, [3]Dipartimento di Scienze della Terra, Università di Firenze, Florence, Italy, [4]Observatorio Volcanológico de Los Andes del Sur (OVDAS), Servicio Nacional de Geología y Minería, Temuco, Chile, [5]Servicio Meteorológico Nacional, Buenos Aires, Argentina

OPEN ACCESS

Edited by:
John Stix,
McGill University, Canada

Reviewed by:
Kimberly Genareau,
University of Alabama, United States
John J Lyons,
U.S. Geological Survey, Alaska, United States

***Correspondence:**
Maurizio Ripepe
maurizio.ripepe@unifi.it

Specialty section:
This article was submitted to Volcanology, a section of the journal Frontiers in Earth Science

Received: *30 June 2020*
Accepted: *04 February 2021*
Published: *24 March 2021*

Citation:
Hantusch M, Lacanna G, Ripepe M, Montenegro V, Valderrama O, Farias C, Caselli A, Gabellini P and Cioni R (2021) Low-Energy Fragmentation Dynamics at Copahue Volcano (Argentina) as Revealed by an Infrasonic Array and Ash Characteristics. Front. Earth Sci. 9:578437. doi: 10.3389/feart.2021.578437

Ash-rich eruptions represent a serious risk to the population living nearby as well as at thousands of kilometers from a volcano. Volcanic ash is the result of extensive magma fragmentation during an eruption, and it depends upon a combination of magma properties such as rheology, vesicularity and permeability, gas overpressure and the possible involvement of external fluids during magma ascent. The explosive process generates infrasonic waves which are directly linked to the outflow of the gas-particle mixture in the atmosphere. The higher the overpressure in the magma, the higher should be the exit velocity of the ejected material and the acoustic pressure related to this process. During violent eruptions, fragmentation becomes more efficient and is responsible for the extensive production of ash which is dispersed in the atmosphere. We show that the phase of intense ash emission that occurred during March 2016 at Copahue volcano (Argentina) generated a very low (0.1 Pa) infrasonic amplitude at 13 km, raising a number of questions concerning the links among acoustic pressure, gas overpressure and efficiency of magma fragmentation. Infrasound and direct observations of the eruptive plume indicate that the large quantity of ash erupted at Copahue was ejected with a low exit velocity. Thus, it was associated with eruptive dynamics driven by a low magma overpressure. This is more evident when infrasonic activity at Copahue is compared to the moderate explosive activity of Villarrica (Chile), recorded by the same array, at a distance of 193 km. Our data suggest a process of rigid fragmentation under a low magma overpressure which was nearly completely dissipated during the passage of the erupting mixture through the granular, ash-bearing crater infilling. We conclude that ash released into the atmosphere during low-energy fragmentation dynamics can be difficult to monitor, with direct consequences for the assessment of the related hazard and management of eruptive crises.

Keywords: fragmentation, infrasound, ash eruptions, volcanic hazard, monitoring

INTRODUCTION

Scientific attention regarding eruptions dominated by ash emission has been increasing since the paradigmatic 2010 Eyjafjallajokull eruption in Iceland (Dellino et al., 2012; Gudmundsson et al., 2012; Cioni et al., 2014). Although the importance of this very frequent type of activity had already been recognized in the stratigraphic records of some volcanoes (e.g. Ono et al., 1995; Andronico and Cioni, 2002; D'Oriano et al., 2011), it was from this Icelandic eruption that research efforts were strongly focused toward many different aspects related to this peculiar type of activity, ranging from the mechanisms of magma fragmentation and transport, through plume and ash dispersal and ash aggregation, to consideration of the wide spectrum of related hazards and their economic and social consequences. These studies largely benefitted from the direct observation and sampling of a few eruptions, for which data derived from geophysical monitoring could be coupled with direct analyses on samples from the observed phases of the eruption (Bonadonna et al., 2011; Miwa et al., 2009; Gaunt et al., 2016; Battaglia et al., 2019). Despite the many efforts dedicated to this topic from the scientific community in the last 10 years, several aspects still remain to be explored and clarified. This is mainly due to the fact that activity dominated by continuous and prolonged ash emission relates to a wide spectrum of mid-intensity eruptive styles (Vulcanian, violent Strombolian, Surtseyan, ash venting) and magma compositions, involving varied processes of magma fragmentation, ash generation and dispersal. For this reason, further studies at volcanoes of different geological and tectonic contexts around the world are needed for better understanding of the main mechanisms driving this type of activity.

Copahue volcano is one of the most active volcanoes in Argentina. Since 2012 it has been characterized by constant passive emissions of steam and SO_2, with frequent episodes of gas and ash emissions that last from a couple of days to months, alternating with phreatic explosions with large emission of water vapor clouds (Global Volcanism Program, 2016, and 2017; Petrinovic et al., 2014; Caselli et al, 2016a; Augusto and Vélez, 2017; Daga et al., 2017). This eruptive activity is generally classified as VEI 2 and poses serious risks to the local population for the large quantity of ash dispersed in the atmosphere (Petrinovic et al., 2014; Caselli et al, 2016b). The area around Copahue is one of the most popular ski resort and thermal areas in Argentina, visited by thousands of tourists every year. The permanent westerly winds blow the ash toward the villages of Caviahue and Copahue, causing problems for traffic circulation and human respiration. Nevertheless, the record of this volcanic activity is very sparse in terms of geophysical data, as well as understanding the explosive dynamics responsible for this large emission of ash.

We present here the first complete infrasound record of a 15 day period (between March and April 2016) during a prolonged (January-April 2016) phase of intense ash-emission activity at Copahue volcano. This eruption was recorded with an infrasonic array and compared with both visible camera and direct observations of the explosive activity, which allow us to relate the infrasonic record to the eruptive style and ash outflux, grain size, componentry, and morphological and textural data collected during certain days of the same period of activity (5 days in February 2016). This information is used in conjunction with infrasound data to constrain the fragmentation process and eruption dynamics.

The infrasonic data were recorded by the first permanent infrasonic array installed in the southern Andes, revealing the weak overpressures associated with ash emission activity compared to phreatomagmatic and/or magmatic activity. The weak overpressure related to the activity at Copahue is demonstrated by comparing these data during the period of the study to a different set of infrasound signals with back-azimuth directions compatible with distal activity at Villarica volcano in Chile, 193 km from the CPH array. The capability to detect signals at large distances confirms the high potential of this infrasonic array as a remote system to monitor activity from many volcanoes of the Andean Southern Volcanic Zone.

COPAHUE VOLCANO

The Copahue-Caviahue Volcano Complex (CCVC) is part of the Caviahue-Agrio caldera (Bonali et al., 2016). It is located in the Southern Andean Volcanic Zone (37°–41,5°) and straddles the border between Argentina and Chile (**Figure 1**), approximately 30 km east of the N-S to NNE-SSW-trending volcanic arc (Melnick et al., 2006; Folguera et al., 2016). Copahue volcano is an active andesitic to basaltic andesitic stratovolcano nested on the western rim of the caldera (Linares et al., 1999). It is elongated in the NE direction and has an elevation of 2,997 m a.s.l. On its summit, nine craters are aligned N60°E (Naranjo and Polanco, 2004); only the easternmost crater is currently active. This active crater has a nearly circular shape of 300 m by 250 m, a depth of 90 m, and contains a nearly permanent, hot hyperacidic crater lake, active at least from 1937 (Caselli et al., 2016b; Agusto and Vélez, 2017).

At least 13 eruptions have occurred during the last 260 years. Despite the scarce detailed historical information, available reports and data suggest low magnitude phreatic and phreatomagmatic eruptive styles over the last two centuries (Martini et al., 1997; Naranjo and Polanco, 2004), whereas the most recent eruptive events in 2000 and 2012 have been mainly Strombolian, with a phreatomagmatic opening phase followed by the occurrence of repeated magmatic pulses (Caselli et al., 2016a). In July 2012, a new eruptive cycle began, with the occurrence of a phreatomagmatic eruption which expelled material from the volcanic conduit at the bottom of the crater lake, accompanied by juvenile material (Caselli et al., 2016a; Daga et al., 2017). In December 2012 the main phase of the phreatic/phreatomagmatic eruption culminated after several hours with a magmatic phase. The crater lake drained during the eruption, and activity changed to small explosions and fumarolic emissions. Reactivation of the explosive activity in 2012 led to the formation of permanent fumaroles, the evaporation of water, and even the expulsion of water in the form of lahars (Caselli et al., 2016a). A small crater lake reformed and was present until November 2015 (GVP, 2013; Agusto and Vélez, 2017). Until early 2017, the volcano

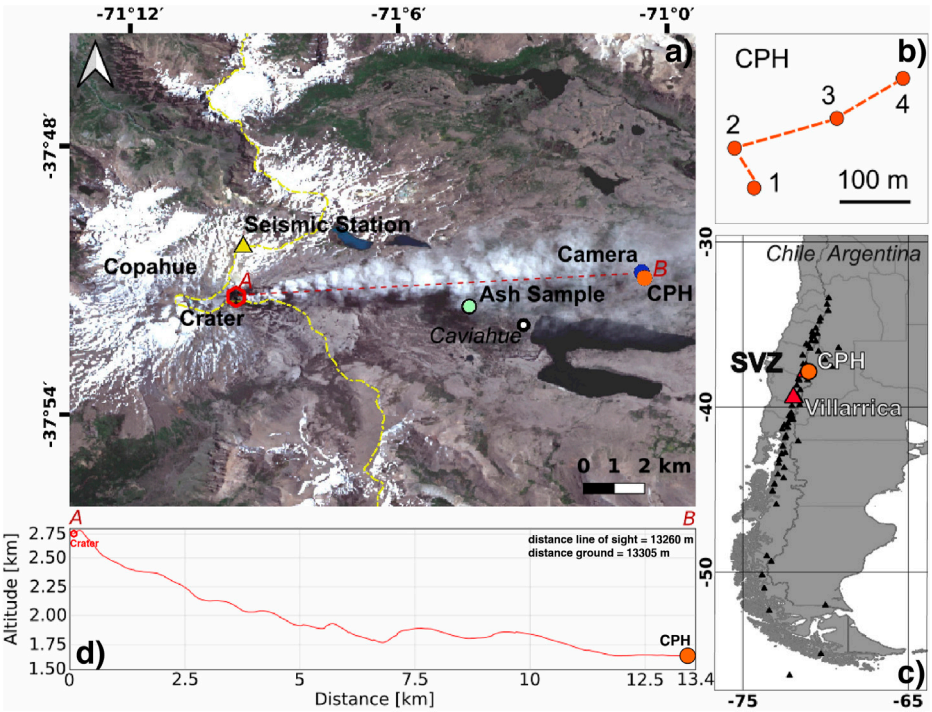

FIGURE 1 | (A) Map showing the locations of the infrasonic array (CPH, orange circle), videocamera (blue circle), ash sample (green circle) and seismic station (yellow triangle) relative to Copahue volcano, where the large ash-rich plume emitted during the 2016 eruption is dispersed by the eastward-directed winds. **(B)** Geometry of the CPH infrasonic array. **(C)** Map of South America showing the locations of Copahue volcano (orange circle) and Villarica volcano (red triangle). **(D)** Topographic section between the Copahue vent and CPH infrasonic array with the topographic information used to evaluate the Fresnel number N.

experienced constant seismic activity associated with emission of gas and ash, with occasional explosions leading to visible nocturnal incandescence (Caselli et al., 2017a). This activity represents a serious risk to the population living around the volcano, both in Argentina and in Chile. In the 2012 eruption, the volcanic plume drifted up to 350 km away from the source (Caselli et al., 2016a), demonstrating that even during these low intensity events, the large quantity of ash dispersed in the atmosphere (**Figures 1A**, **Figure 2**) can also represent a major problem for civil aviation (Bonadonna et al., 2012).

The February-March 2016 Activity of Copahue

The vent area of Copahue was characterized from the end of November 2015 by the presence of a small cone within the crater, and by a nearly empty crater lake (**Figure 2B**; GVP, 2016; Agusto et al., 2017). The cone was still present in the first weeks of February 2016, together with a small lake inside the main crater. The period February–March 2016 was characterized by continuous and quite constant activity (**Table 1**), which continued the trend of activity of December 2015-January 2016 (Caselli et al., 2017b). Seismic tremor was higher than normal, reaching its highest amplitude since 2012 (**Figure 3**) on March 3th (OVDAS-SERNAGEOMIN, 2016a), although generally maintaining an intermediate level (reduced

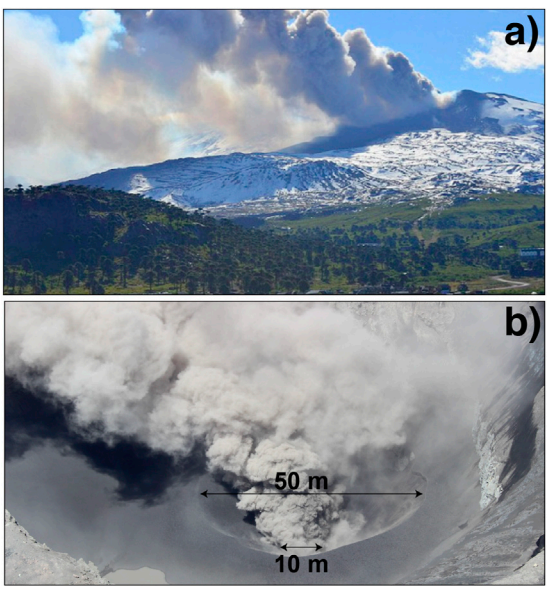

FIGURE 2 | (A) Large ash-rich plume emitted during the 2016 eruption is dispersed by the eastward winds. During this type of activity, the ash plume is bent to the east by the wind immediately above the crater, revealing a weak gas thrust phase driven by a slow ascent rate. **(B)** Size of crater rim and vent at Copahue volcano; the photograph was taken in March 2016.

TABLE 1 | Summary of geophysical and observation data related to the January-April 2016 activity at Copahue volcano. Data from "Reporte de Actividad Volcánica (RAV), Regiòn del Biobío," OVDAS-SERNAGEOMIN (http://sitiohistorico.sernageomin.cl/lista-region-8.php).

Month	January 2016		February 2016		March 2016		April 2016
Days	1–15	16–31	1–15	16–29	1–15	16–31	1–15
VT	68	28	15	9	7	12	33
LP/VLP	51	41	13	17	16	42	29
Tremor	Constant, intermediate level (RD < 1.8 cm^2)	Constant, intermediate level (RD < 4 cm^2)	Constant, intermediate level (RD < 4 cm^2)	Constant, intermediate level (RD < 5 cm^2)	Constant, intermediate level (RD < 5 cm^2)	Constant, intermediate level (RD < 3 cm^2)	Constant, intermediate level (RD < 3 cm^2)
Mean SO_2 (t/day)	691 ± 184	724 ± 91	753 ± 199	1,125 ± 176	693 ± 128	853 ± 189	921 ± 37
Max SO_2 (t/day)	2,573 January 12	1,380 January 16	2,735 February 13	4,264 February 25	2079 March 8	2,830 March 23	2,323 April 4
Activity	Continuous ash emission, gray plume, incandescence	Continuous ash emission, gray plume, incandescence	Continuous ash emission, gray plume, incandescence	Continuous ash emission, gray plume, incandescence	Continuous ash emission, gray plume, incandescence	Continuous ash emission, gray plume, incandescence	Continuous ash emission, gray plume, incandescence
Max plume height (above the vent)	850 m January 13			1,250 m		1,500 m March 22	

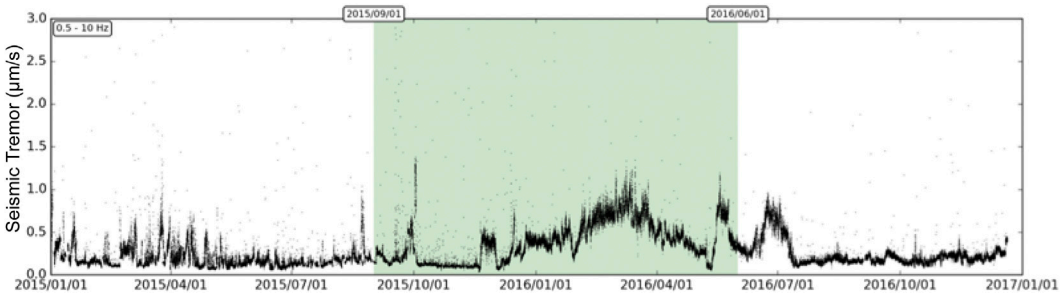

FIGURE 3 | Seismic tremor calculated at the Copahue station located 2.1 km from the crater in the frequency band 0.5–10 Hz. Tremor amplitude shows a gradual but clear increase from the end of 2015 and reaches the maximum amplitude during March 2016 (green area).

displacement RD variable between 3–5 cm^2, **Table 1**). During the entire period a low-level ash plume was present up to ~1,000 m above the vent and generally traceable by satellite up to distances of 50–100 km to the SE-ESE. Incandescence in the vent area was visible at night from a videocamera located at 13 km from the vent (**Figure 1A**). Minor peaks in activity possibly occurred with peaks in SO_2 flux (25 February, 23 March) and with the formation of slightly higher ash plumes up to 1,500 m (**Table 1**) (OVDAS-SERNAGEOMIN, 2016a).

During March and the beginning of April, a videocamera showed a constant emission of ash and gases, as well as nocturnal incandescence occurring in the crater. This activity was directly related to a small increase in tremor recorded by the seismic stations **(Figure 3)**. From March 23 to 26 the plume reached a maximum height of about 1,500 m above the vent (GVP, 2016, OVDAS-SERNAGEOMIN, 2016a).

Visual observations on March 25 reported the emission of ash and gases, intermittently with clouds of water steam and the ejection of volcanic bombs coming from the cinder cone inside the crater. A small lake inside the crater and bombs ejected as far as 240 m from the vent were also observed. At the time, the rim of the cone within the crater was 50 m high, and the active vent was ~10 m wide (**Figure 2B**).

The seismicity, SO_2 flux and the description of volcanic activity (**Table 1**) of the entire period were compiled in reports from OVDAS-SERNAGEOMIN (2016a), which explains this kind of activity as the result of interaction of pockets of magma at shallow depth with the surficial hydrothermal system.

THE INFRASOUND ARRAY

On February 2014 the first permanent infrasound array in the Southern Andes for monitoring volcano activity was installed near Copahue volcano. The array is located 13 km east of the active crater and at 1,660 m above sea level (**Figure 1A**). It consists of four elements arranged in a L-shape geometry with an aperture of ~200 m **(Figure 1B)**. Infrasound is recorded by

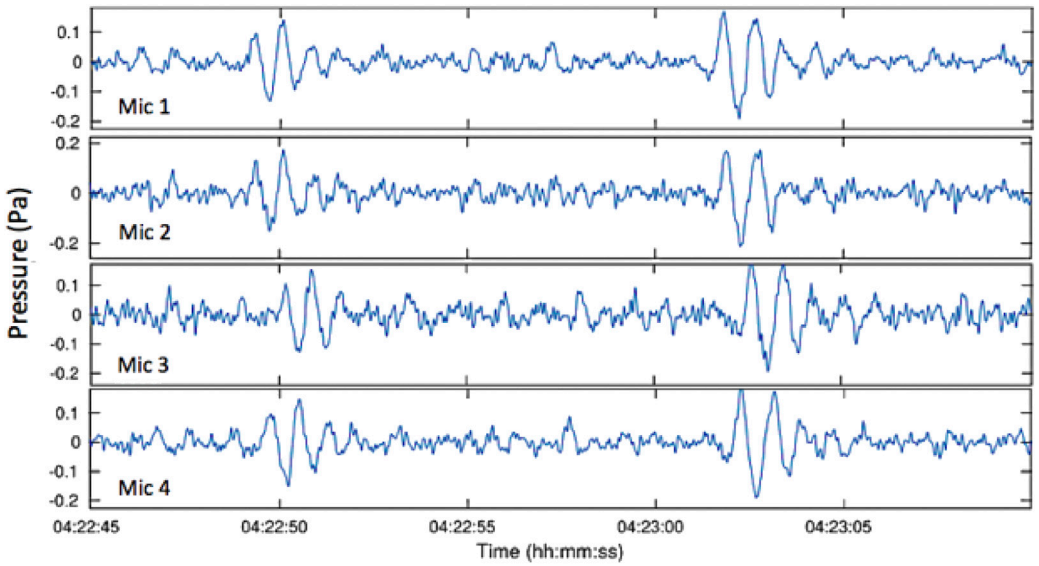

FIGURE 4 | Example of infrasound recorded at the different microphones of the array during March 22, 2016. Signals were filtered between 0.5 and 10 Hz and show clear impulses of short duration with small pressure amplitude (0.2 Pa) repeating every 14 s, which are associated with explosive activity at Copahue.

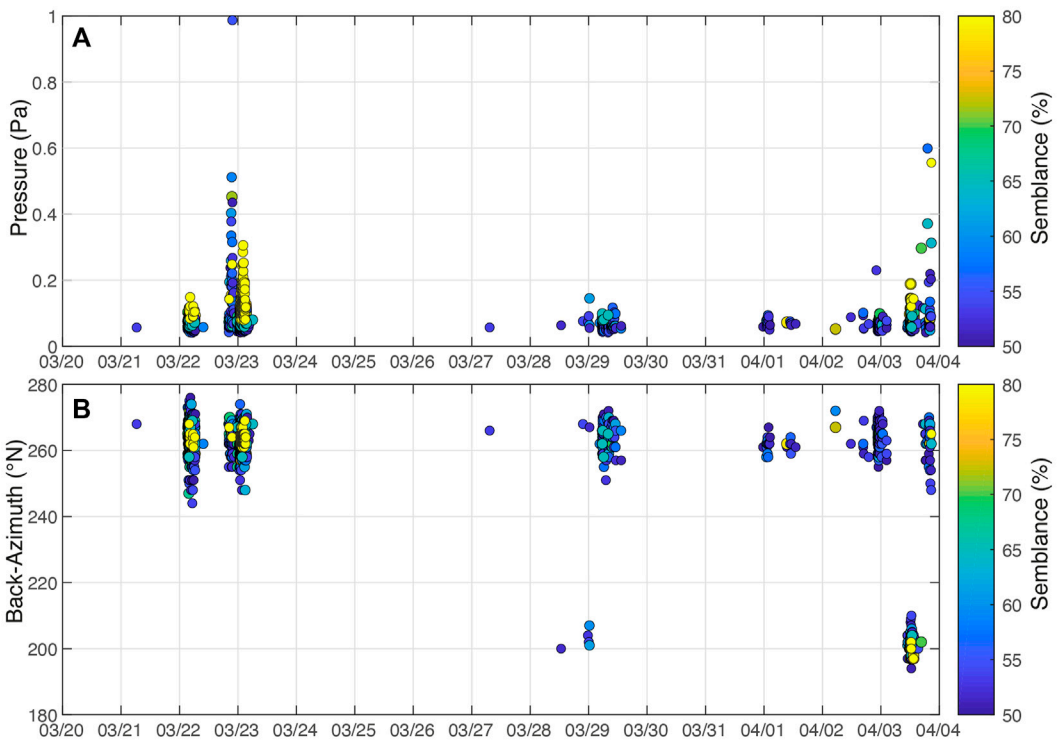

FIGURE 5 | (A) Acoustic pressure; **(B)** backazimuth detected by the array with semblance >50% during the period 20 March and 4 April 2016; the color bar indicates the semblance value. Explosive activity at Copahue volcano is identified by the signals coming from ~260°N with amplitude rarely above 0.3 Pa. Detections with backazimuth around 200°N on March 29 and April 3, are instead related to the explosive activity at Villarrica volcano (Chile).

analog differential pressure transducers with a sensitivity of 25 mV/Pa in the frequency range from 0.01 to 100 Hz, with noise level of 50 dB at 1 Pa^2/Hz. In order to minimize the impact of the wind on the sensors, the array was deployed in a moderately forested area. Each sensor is connected by cable to a six channel 24-bit digitizer (Guralp CMG-DM24) that records

and stores data at a sampling rate of 100 samples per second. Data are then transmitted via internet through TCP/IP protocol to the Laboratorio di Geofisica Sperimentale, University of Florence in Italy, the University of Rio Negro in Argentina, and OVDAS in Chile, where they are processed in real-time.

Infrasound Array Processing

Infrasonic arrays are typically used to investigate the acoustic wavefield. Among several different methods, multi-channel correlation analysis (e.g., Ripepe and Marchetti, 2002), used for calculating coherence among different stations of the array as a function of the receiver-to-source propagation back-azimuth, was applied to the CPH infrasound data. The multi-channel correlation analysis is based on the assumption that a signal is coherent at different elements of the array, and it is applied to infrasonic data filtered in the 0.5–10 Hz frequency band (**Figure 4**). Array analysis is performed in real-time on a 5-second moving window, with an overlap of 1 s. The result of this processing is represented in terms of temporal variation of the semblance as a function of the back-azimuth direction (Ripepe et al., 2007). For each signal with semblance (semblance measures the amount of similarity between infrasound traces) higher than 50%, the back-azimuth and the mean acoustic pressure recorded at the array are calculated (**Figure 5**).

Limitations of the array detection techniques are related to the signal-to-noize ratio, which depends on the local infrasonic noise mainly due to strong wind, as well as on the attenuation of the wavefield during propagation in the stratified atmosphere (de Groot-Hedlin et al., 2008; Garcés et al., 2008; Lacanna et al., 2014) and along the ground from the source to the receiver path (Lacanna and Ripepe., 2013).

INFRASOUND MONITORING AT COPAHUE

During the February–March 2016 period, infrasonic activity was generally low, and only rarely did the array locate coherent signals associated with explosive events (**Figure 5**) and ash emissions. On March 21, 2016 at 6:09 UTC, array processing reveals coherent small acoustic signals with amplitude between 0.05 and 0.2 Pa propagating with a back-azimuth of ~266°N, corresponding to the direction of the active crater (**Figure 5**). These coherent acoustic signals were characterized by impulsive transients with a mean duration of 1.5 s and frequency of 1.12 Hz, typical of moderate explosive activity, or overpressurized magma degassing (**Figure 4**). These acoustic signals are similar to those associated with explosive activity observed at other volcanoes (Johnson 2003; Johnson and Ripepe 2011; Fee and Matoza 2013; Ripepe et al., 2018), but characterized by low pressure amplitude (p) generally around 0.2 Pa (**Figure 4**), which when reduced at r_o = 1 km from the source is equivalent to 2.6 Pa ($pr = p(r/ro)$), where r is the distance (13 km) between the array and the crater. For comparison, Stromboli volcano generates infrasonic transients with frequency content between 2–4 Hz and amplitudes (p) between 20–50 Pa at r_o~0.5 km from the source (e.g., Lacanna and Ripepe 2013; Delle Donne et al., 2016) which converts to a reduced pressure (P_r) of 10–25 Pa at 1 km.

The low amplitude transient acoustic signals of the initial eruptive phase became more frequent and finally merged in a continuous oscillation (**Figure 6**) approaching the more violent eruptive phase on March 23 (**Figure 5**). These oscillations are quasi-monochromatic (**Figure 6**) at around 1.2 Hz (**Figure 7**) and highly coherent (semblance>80%) among the infrasonic sensors of the array reaching maximum amplitudes of ~1.0 Pa on March 23 (**Figure 5**). This phase coincided with the maximum emission of ash, generating a plume that reached a height of 1,500 m above the volcano (4,350 m a.s.l.). The ash plume was visible on satellite imagery, and at 12:10 UTC on 23 March 2016, ash was traveling eastward at a distance of 37 km from the volcano (**Figure 1A**). This activity caused the Volcanic Ash Advisory Center (VAAC) of Buenos Aires to issue a notification of volcanic ash dispersion for Copahue volcano. The same VAAC reported ash drifting to a distance of 150 km (GVP, 2016). In spite of the different magma composition, similar infrasonic behavior has been observed during more energetic lava fountaining at Etna volcano in Italy. At Etna, explosive eruptions are in fact preceded by violent Strombolian activity associated with a rapid sequence (every 2 s) of large infrasonic transients (P_r = 20–30 Pa at 1 km) which merge to continuous acoustic pressure oscillations of 0.7 Hz during a sustained eruptive column (Ulivieri et al., 2013).

Infrasonic activity with back-azimuth coherent with the direction of the active crater (~266°N) was also detected after March 23 but was characterized by only a few events randomly distributed and seldom exceeding 0.12 Pa. Infrasound during this phase is most probably associated with a weak Strombolian phase as evidenced by the incandescent volcanic bombs observed at night.

Explosive Activity at Villarrica Volcano, Chile

On april 3, 2016, at around 10:57 and 14:23 UTC, array processing shows several detections which are highly coherent (>70%) with back-azimuth at around 200°N (**Figure 5B**) and acoustic pressure ranging between 0.2 and 0.06 Pa (**Figure 5A**). A close analysis of the back-azimuth plot reveals that similar detections were identified by the array with the same back-azimuth several days beforehand on March 28 at 11:46 (**Figure 5**).

Infrasonic activity with a back-azimuth of ~200°N points to the position of Villarrica volcano, located 193 km from CPH array (**Figure 8**) and showing a frequency content ~0.8 Hz (**Figure 7**) which falls into the infrasound frequency range of 0.5–2 Hz previously recorded at Villarrica (Ripepe et al., 2010; Goto and Johnson 2011). These detections coincide with moderate explosive activity occurring on april 3, characterized by an ash column ~300 m high and thermal anomalies detected by satellite (OVDASSERNAGEOMIN, 2016b), abril vol. 04). Even though Villarrica is almost 15 times farther from the array than is Copahue, the amplitude and waveform of infrasound generated by the two volcanoes are comparable (**Figure 9**). However, explosive activity at Villarrica produced acoustic pressure, which when reduced at 1 km from the crater gives amplitudes larger than 25 Pa. This value is one order of magnitude larger than Copahue and comparable to values recorded during ordinary explosive activity at Stromboli (Lacanna and Ripepe 2013; Delle Donne et al., 2016),

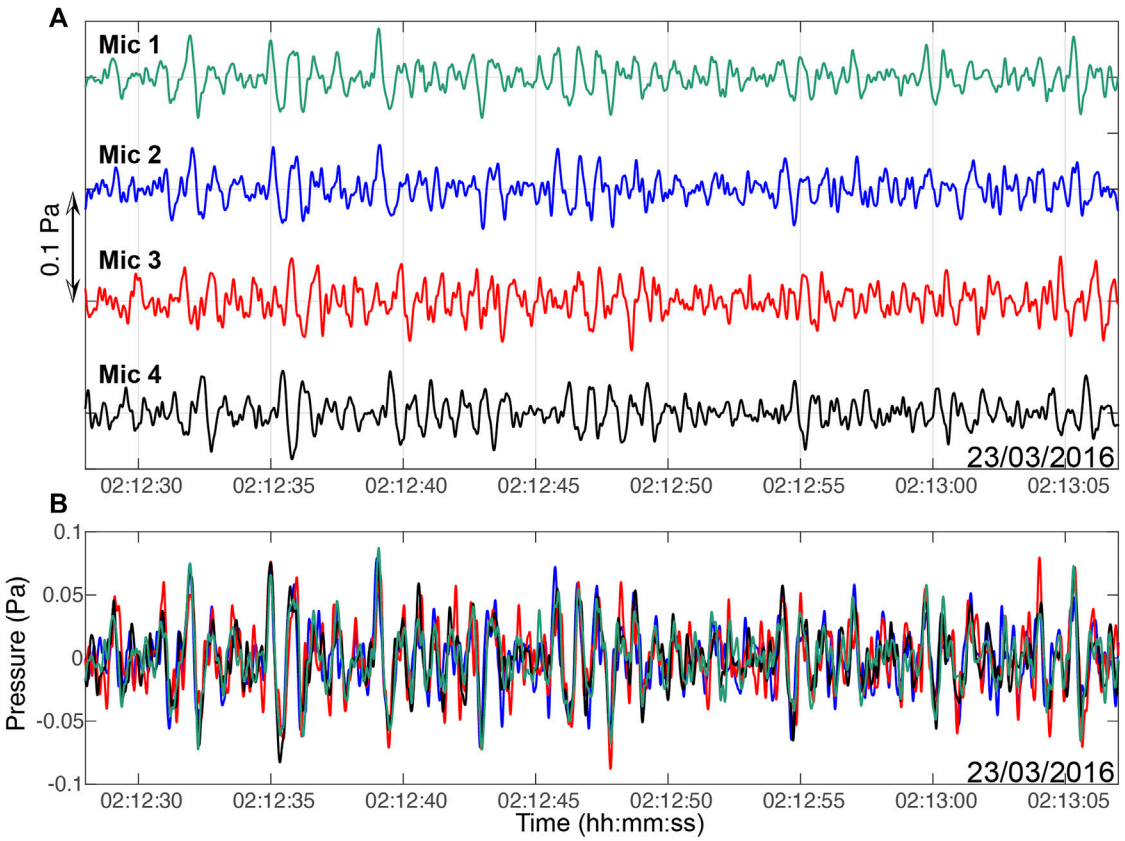

FIGURE 6 | (A) Example of infrasonic signals recorded at four sensors of the array during the most intense ash eruption phase. **(B)** Time shifted infrasound signals related to Copahue activity show continuous quasi-monochromatic oscillation at 1.2 Hz which is coherent across the array.

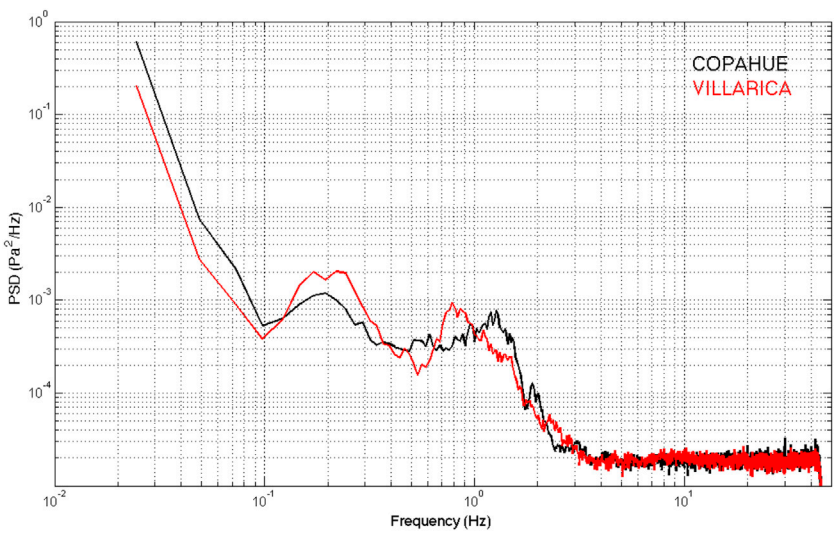

FIGURE 7 | Power density spectrum of infrasonic signals recorded by the CPH array relative to Copahue (black line) and Villarrica (red line) volcanoes. Note that Villarrica has a slightly lower frequency content at around 0.8 Hz compared to Copahue at 1.2 Hz. Both spectra show energy at around 0.2 Hz (5 s), which is typical of atmospheric microbaroms.

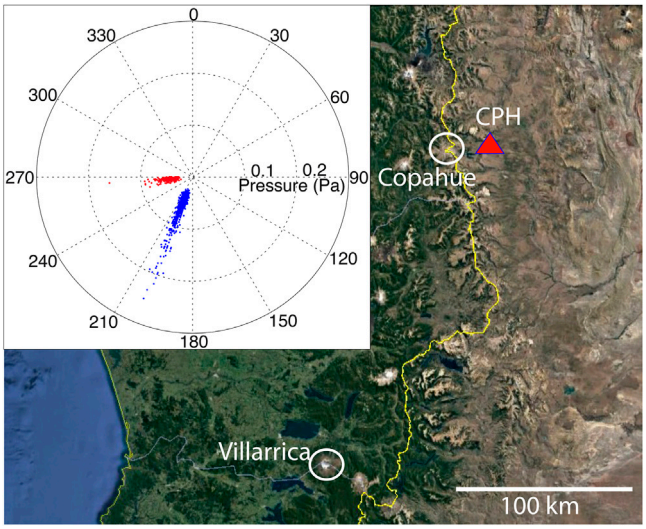

FIGURE 8 | In the inset, the back-azimuth of pressure distribution for March 23 (red dots) and April 3, 2016 (blue dots) reveals two sources located at 266°N and 203°N, which coincide with the positions of Copahue (red) and Villarrica (blue) volcanoes, respectively.

indicating the extremely weak pressure excess associated with the ash-rich explosive activity at Copahue.

CHARACTERISTICS OF THE ASH FRAGMENTS ERUPTED FROM COPAHUE

In order to investigate the processes controlling ash production and emission during the constant activity of February–April 2016 at Copahue, ash samples were collected in dedicated plastic containers while falling during a 5-day sequence of activity from February 19 to 23, 2016, during this prolonged eruptive period of activity. Unfortunately, we could not directly sample falling ash during the same days of the studied infrasound record. However, the activity of Copahue during the period of ash collection was comparable to the activity observed in March and recorded by the infrasound array (GVP, 2013; **Table 1**). The collection site (**Figure 1A**) and the analytical methods (grain size, ash textures and morphology) used for the study of the ash are reported in the **Supplementary Material** (**Supplementary Table S1**), while results of ash characterization are reported in **Figure 10**.

Ash samples show a well sorted, nearly symmetric, leptokurtic (kurtosis value always greater than 1) grain size distribution with a mode between 2.5 and 3.5 phi and a very small content of fine ash (less than 10 wt% > 4 phi; **Figure 10A**). Componentry of the ash is constant throughout all the sampled activity and distributed in similar proportions among three different components (**Figure 10B**): transparent, vitric shards and micropumices (JUV; abundances between 32 and 39%); opaque, black, dense to vesicular, variably glass-bearing clasts (REC; between 36 and 38%); and loose crystals (CRY; between 22 and 30%). Sparse, hydrothermally altered lithic fragments (HYD in **Figure 10**), from yellow to pinkish in color, are occasionally present, but with very low relative abundances never exceeding 1%.

JUV clasts (**Figures 11A–C**) are characterized by fresh, nearly microlite-free glass and by an intermediate vesicularity (35–50 vol %), characterized principally by isolated, unconnected, small (50–200 microns in diameter) rounded vesicles (**Figure 11B**). The external surfaces of the particles are jagged, due to multiple intersections with vesicles. Intersections with the largest vesicles (mean diameter around 400–500 microns) result in smooth, concave external surfaces of the clasts (**Figure 11C**). Fluidal

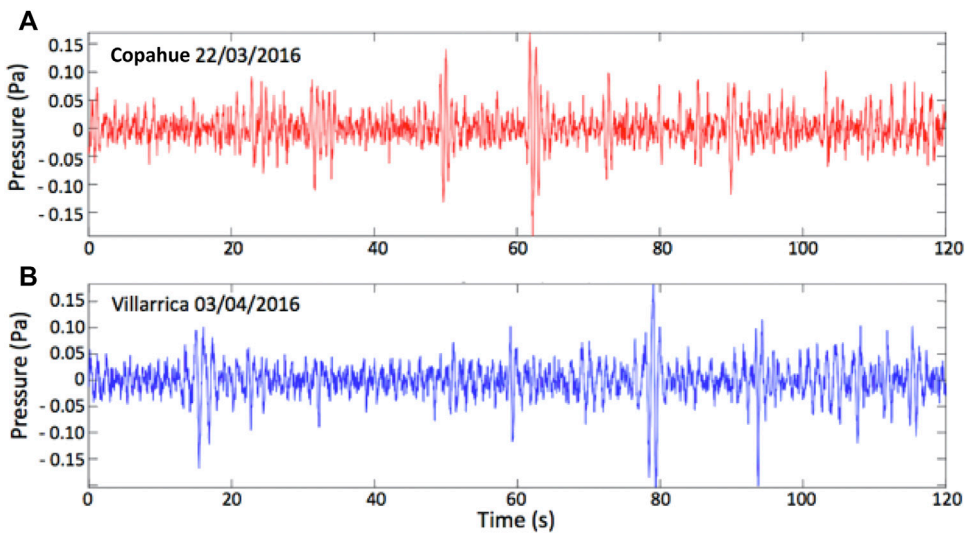

FIGURE 9 | (A) Infrasonic signal recorded on March 22 (red signal). **(B)** Infrasonic signal recorded on April 3 (blue signal). Both signals have similar acoustic amplitude, but array analysis reveals different back-azimuth directions from ~266°N (a, red signal) and ~200°N (b, blue signal). These two different back-azimuth directions are compatible with the location of **(A)** Copahue and **(B)** Villarrica.

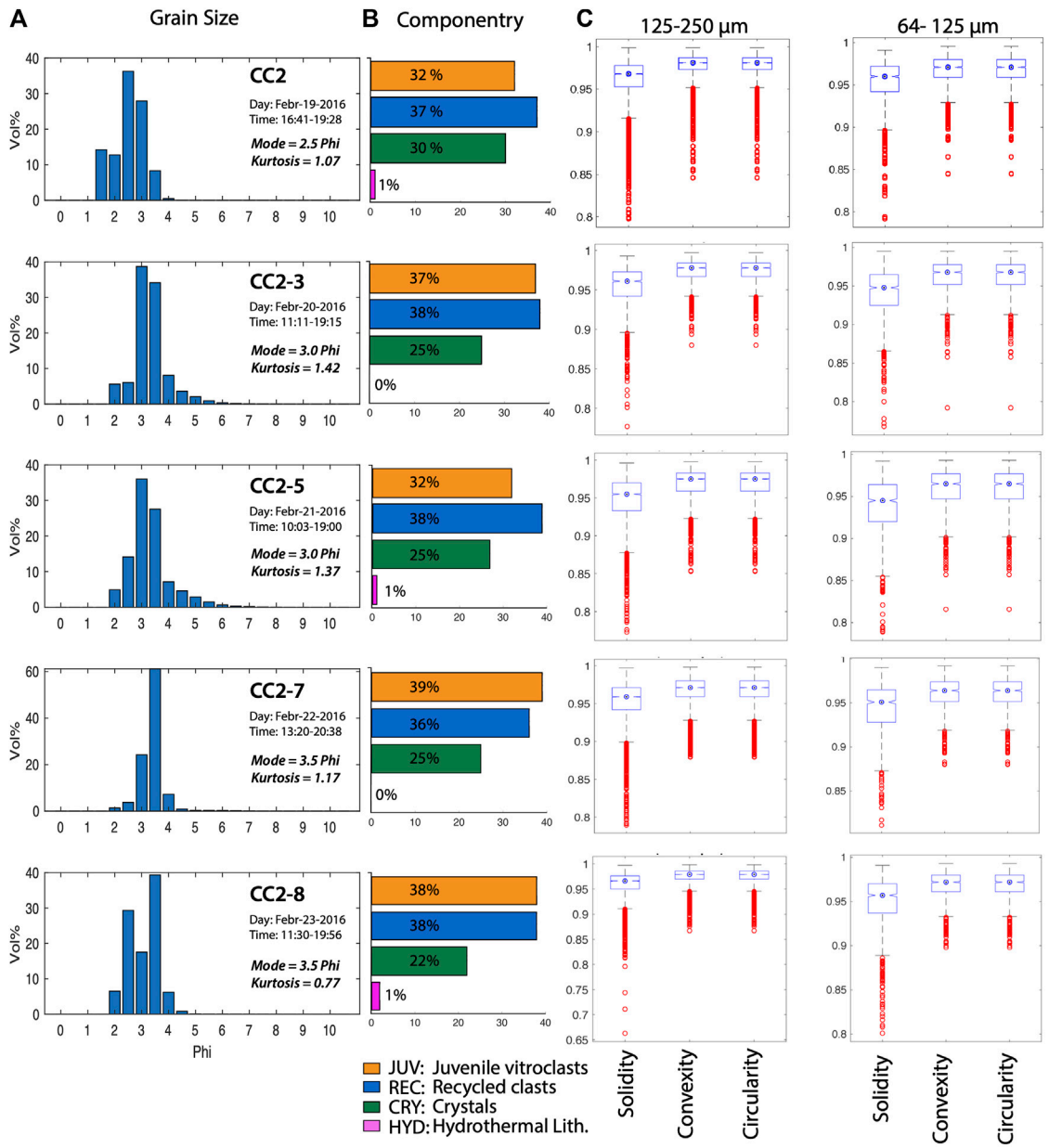

FIGURE 10 | Grain size **(A)**, componentry (500–250 µm fraction; **(B)** and shape parameters **(C)** for the studied ash samples (*Solidity* = Particle Area/Convex Hull Area; *Convexity* = Convex Hull Perimeter/Particle Perimeter; *Circularity* = 4 π Particle Area/(Particle Perimeter)^2; further details on ash analysis are provided in the **Supplementary Materials**.

surface textures, typical of the activity related to the initial, higher intensity phase of the 2012 eruption (Caselli et al., 2016; Daga et al., 2017), have not been recognized in the analyzed samples. JUV clasts are here considered to result from the primary fragmentation of juvenile magma driving the eruption.

REC clasts (**Figures 11D–G**) consist of variably vesicular, variably crystallized clasts which generally exhibit blocky equant morphologies, with more regular shapes compared to JUV. Polished sections of these clasts typically reveal a highly crystallized groundmass (**Figures 11E–G**). Two distinct populations of microlites are identifiable in terms of size. The first is represented by sparse, euhedral and very elongate microlites of plagioclase (20 µm), typically characterized by skeletal textures and, for this reason, interpreted as possibly related to degassing-induced crystallization of magma before fragmentation. The second population is formed by Fe-Ti oxides and plagioclase crystals typically smaller than 5 µm in size that are characterized by a strong interface-controlled growth and dendritic to plumose textures (**Figure 11F**). They are mainly found along the contact between groundmass glass and the

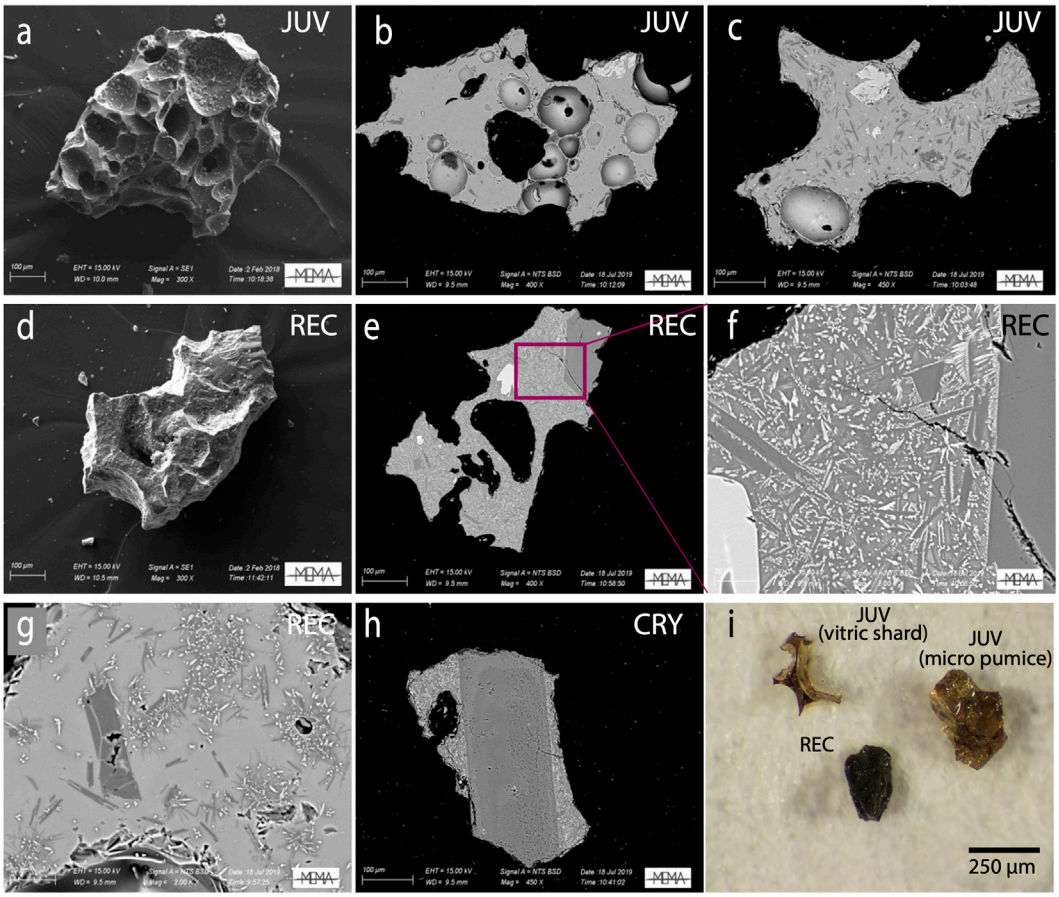

FIGURE 11 | Different types of ash fragments; **(A–C)** secondary and back-scattered electron images of juvenile ash (JUV), characterized by angular vesicular fragments with glass-rich groundmass; **(D–G)** secondary and back-scattered electron images of lithic fragments (REC), characterized by an overall shape similar to the juvenile component, rough surfaces related to fine particle sintering, and a variable, finely microlitic growth typical of ash recycling in a hot environment; **(H)** loose plagioclase crystal (CRY) showing evidence of recycling on the adhering glass; **(I)** optical microscope image of the different ash components.

micro-phenocrysts, along glass banding horizons, or as sparse spherulitic clusters in the glass (**Figure 11G**). External surfaces of the clasts are generally rough, reflecting the diffuse presence of tiny microlites. The particle vesicularity is generally lower (20–35 vol%) with respect to the JUV component. Bubbles are commonly irregular and deformed, possibly resulting from partial collapse (**Figure 11E**). Similar to what we observe on external surfaces, the inner surfaces of the bubble walls are often very irregular due to diffuse crystallization of microlites in the surrounding glass. All the textural and morphological features recognized in REC clasts correspond to experiments simulating conditions of intra-crateric, high-temperature ash recycling by D'Oriano et al. (2012); D'Oriano et al. (2014) and Deardorff and Cashman (2017). This evidence leads us to interpret this type of clast as recycled fragmented material residing in the crater environment.

Another component of the analyzed ash fraction is represented by broken, typically euhedral, loose crystals (CRY; **Figure 11H**). This class of fragment is dominated by transparent crystals of plagioclase and by minor pyroxene and olivine (representing at maximum 5–10 vol% of the total CRY clasts). Importantly, plagioclase crystals commonly preserve adhering portions of groundmass glass characterized by abundant µm-sized microlites arranged in a dendritic, sometimes plumose texture similar to that observed for the REC component (**Figure 11H**), suggesting also in this case an important secondary reheating (and hence recycling) for a large part of the CRY component.

Clasts of different size were also characterized by their external shape using appropriate shape parameters (Solidity, Convexity and Circularity; see **Supplementary Material** for definition). No significant variations in the average values of the particle shape parameters are observed for the analyzed samples, apart from minor variation in the interquartile spread of these values. These observations apply to the different size fractions of the ash particles.

DISCUSSION

Slow Explosive Dynamics at Copahue

The low pressure associated with the ash eruptions raises important questions for the dynamics of the fragmentation

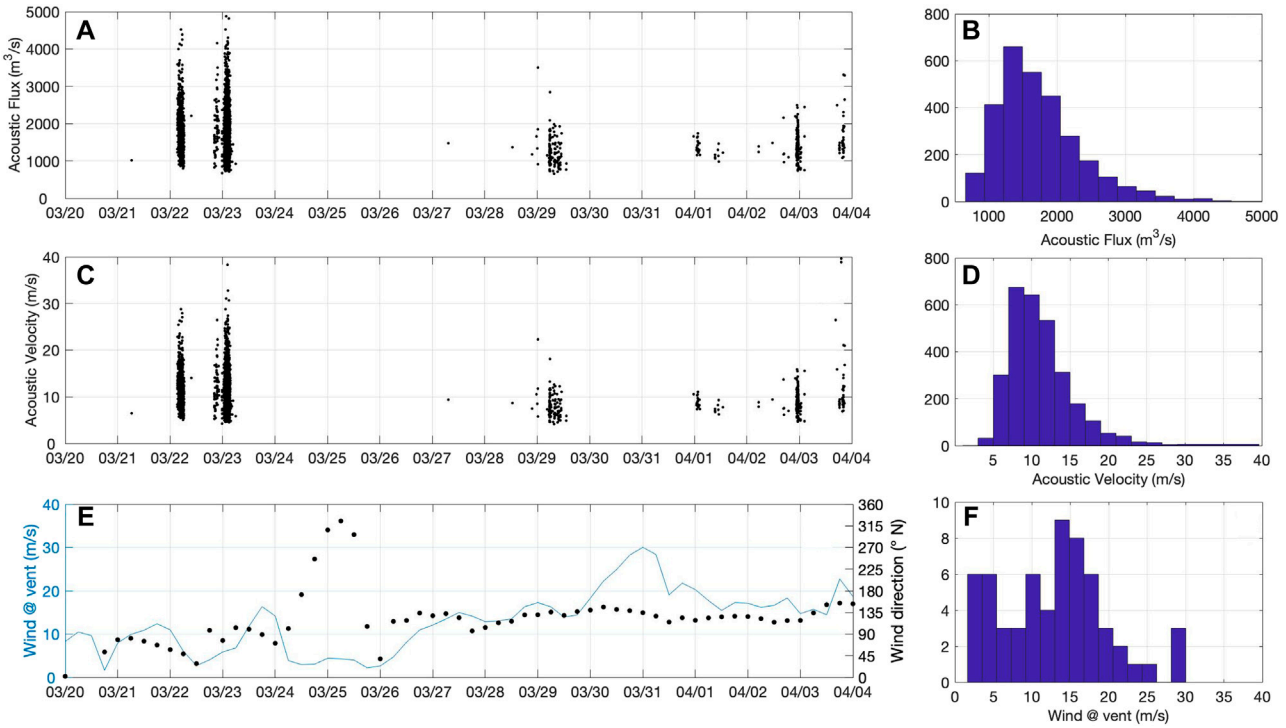

FIGURE 12 | (A) Volumetric flux derived from infrasound records, **(B)** histogram of volumetric flux, **(C)** gas exit velocity evaluated from volumetric flux using a vent surface area of 157 m^2, **(D)** histogram of exit velocity, **(E)** wind velocity and wind direction at 3,000 m a.s.l., which is the altitude of the vent, **(F)** histogram of wind velocity.

process within the conduit of this volcano. In the last 10 years, infrasound records have been applied largely to derive source parameters (i.e., volumetric flux, exit velocity) of volcanic explosions (Ripepe et al., 2013; Kim et al., 2015; De Angelis et al., 2016; Fee et al., 2017). Such parameters relate to the spherical acoustic wavefield, which strongly depends on the conduit radius (a), resulting in different amplitude and radiation patterns for different wavenumbers (k). The acoustic amplitude radiated into the atmosphere depends on the reflection coefficient ($|R|$) at the open-end conduit, whereas the radiation pattern is expressed by the directivity (α) of the acoustic wavefield outside the conduit (Lacanna and Ripepe 2020). Both parameters ($|R|$ and α) depend on the ka value. From field observations we estimated a vent radius a = 5 m (**Figure 2B**) which for a frequency content of 1.2 Hz and acoustic speed c = 340 m/s gives a value of ka = 0.11. This ka corresponds to $|R| = 0.99$ and an isotropic radiation pattern with $\alpha = 1$ (Lacanna and Ripepe 2020).

The above authors suggest evaluating the volumetric flux inside the conduit $q_{i(t)}$ (**Figures 12A,B**) using the infrasonic waveforms $p(t)$ corrected for conduit geometry and scattering effects caused by topography through the insertion loss (IL) as follows:

$$q_i(t) = \frac{2\pi r}{(1+|R|)\rho\alpha 10^{\left(\frac{IL}{20}\right)}} \int_0^t p\left(t+\frac{r}{c}\right)\mathrm{d}t, \qquad (1)$$

where ρ = 1.1 kg/m^3 is the air density and r = 13320 m is the distance from the source. The Insertion Loss (IL) depicts the efficiency of a barrier in reducing the acoustic amplitude and is expressed as a function of the Fresnel number N (Maekawa, 1968):

$$IL = 10\log_{10}(3+20N). \qquad (2)$$

Using the topographic section information between vent and infrasonic array, we estimated a Fresnel number of N = 0.3 (**Figure 1D**) and consequently an IL = −9.5 dB. The volumetric flux calculated for the entire dataset ranges between 0.8 × 10^3 and 4.8 × 103 m^3/s with a mean flux of 1.7 × 103 m^3/s (**Figures 2B**, **12A**), which for a conduit surface $S = 2\pi a^2$ = 157 m^2 gives a mean plume exit velocity of 11 m/s (**Figures 2D**, **12C**).

This low value for the exit velocity is in agreement with the weak dynamics of the ash plume, which is generally observed to bend immediately above the crater (**Figure 2A**) during low wind speed (50 m/s) conditions (**Figure 12**; **Table 1**). The acoustics and visual observations thus suggest that the explosive activity of Copahue volcano is characterized by a low-velocity release of the ash-gas mixture from the vent, most probably driven by a low pressure. This conclusion is in apparent contrast with the large quantity of ash characterizing the eruptive plume during this phase. Infrasound thus suggests that ash-rich explosive activity at Copahue is related to efficient magma fragmentation/transport processes operating at a low-energy regime, hence posing some important questions on the nature of the fragmentation process.

Inferences on Magma Fragmentation Processes

The nearly invariant textural and morphological features of the ash cargo deposited by the plume confirm a generally constant mechanism of ash production and recycling during the investigated 5 days-long activity. In agreement with the available descriptions of the activity during the first months of 2016 (**Table 1**), we suggest that similar conditions of ash fragmentation/recycling persisted during the entire period. Ash morphology and componentry can provide some basic hints about the mechanisms of magma fragmentation and eruption.

While magma-water interaction has often been suggested as a main driver of magma fragmentation at Copahue (Naranjo and Polanco, 2004; Petrinovic et al., 2014; Daga et al., 2017), we do not consider this process to be significant based upon the ash characteristics and infrasound signals. Ash, in fact, does not present any textural or morphological features recognized as typical of this mechanism of fragmentation (absence of an important ash aggregation; no surface cracks or alteration of the ash fragments). Moreover, the very low amplitude of the pressure transients recorded in the infrasonic signals are not in agreement with explosive activity driven by magma-water interaction, which should be accompanied by important pressure peaks generated by the impulsive, rapid vaporization and expansion of vapor created by the water-magma contact (Fee and Matoza, 2013; Wohletz et al., 2013). In addition, processes such as rapid dissipation of overpressure related to the presence of a surface water body (as for example observed at White Island volcano, New Zealand, when activity was characterized by near-continuous pulses of gas, ash emissions with low exit velocities, and generation of very weak plumes; Houghton and Nairn, 1991) cannot be invoked at Copahue, where the monitored activity was preceded by a large reduction and then disappearance of the water in the crater lake (**Figure 2B**).

The abundant presence of clasts showing evidence of thermally induced post-fragmentation recrystallization of the glass, represented by the REC and at least part of the CRY components (overall reaching up to 60–70% of the total), clearly demonstrates that a large portion of the ash dispersed by the plume was not produced directly by syn-eruptive fragmentation. The impulsive, high-frequency nature of the activity revealed by the infrasonic signal (**Figure 4**) and by the billowing shape of the associated plumes (**Figure 2A**), suggests an unsteady character of the emission, typical of low-intensity activity. Conditions of continuous ash recycling in the crater area are generally favored during this type of activity (Houghton and Smith, 1993; D'Oriano et al., 2014). On the other hand, the textural and morphological features of the JUV fraction of the ash (sharp external edges; absence of fluidal shapes) suggest formation by rigid fragmentation of a mildly to low vesicular magma with a poorly developed permeability (absence of very large, deformed or coalescing vesicles) that rapidly ascends in the conduit under nearly closed degassing conditions (absence of groundmass microlites related to degassing-induced crystallization).

Explosive, rigid magma fragmentation can occur under different conditions, and it is generally associated with release of overpressure which mainly depends on the textural properties such as vesicularity and permeability, and on the rheology of the magma (Spieler et al., 2004; Kueppers et al., 2006; Cashman and Scheu, 2015). For intermediate values of vesicularity (40–50 vol%, similar to those observed in the JUV component), this overpressure is close to a minimum and measured on the order of 2–4 MPa (Spieler et al., 2004; Kremers et al., 2010). As a general rule, the gas-ash mixture generated at fragmentation accelerates in the conduit, and its passage through an empty crater can result in its progressive decompression by expansion of the erupting mixture, finally increasing the velocity of the jet entering the atmosphere (Woods and Bower, 1995). Conversely, for the activity observed at Copahue, the low exit velocity of the eruptive mixture, as testified by both the infrasound monitoring and the direct observation of the plume, can be considered as an indication of its arrival at the surface under low-pressure conditions. We suggest here that these peculiar eruptive conditions can result from the combination of two predisposing effects: a magma texture and rheology requiring a low overpressure for fragmentation coupled with an attenuating effect related to the passage of the erupting mixture through an ash-filled environment. In particular, the entrainment and subsequent transport of some of the ash which had been continuously accumulating at the crater base can be described as a process of elutriation following partial fluidization of the crater base infill. Assuming a thickness of 10 to 30 m for the ash-enriched zone at the crater base, a pressure drop on the order of 1 to 5 bars can be estimated through the application of the Ergun equation (Cocco et al., 2014), confirming an important damping effect upon the pressure of the ascending mixture. These combined effects can thus explain the low amplitude of the infrasonic signal recorded at Copahue during this type of activity. The identification of recycled, hot material in the products of continuous ash emission is not simply an academic exercise. While on one side the presence of previously erupted ash in the crater can exert an important damping effect to the passage of the gas-driven eruptive mixture (hence decreasing pressure and exit velocity), on the other, the textural characteristics of this material clearly indicate a high temperature state. We suggest that the still large heat content of the recycled ash can have an important effect on the atmospheric evolution of the eruptive plume, enhancing its convective capability. This effect should be studied and quantified in detail by further studies.

CONCLUSION

The mechanisms controlling eruption dynamics and the shifts in eruptive style at volcanoes characterized by prolonged, low to mid-intensity ash emission are generally poorly known. Integration of infrasound data and observations on the ash erupted during the same activity can provide important hints

regarding these mechanisms. Eruptions from Copahue volcano are generally a source of a large quantity of ash, so that understanding the processes of magma fragmentation, eruption, atmospheric injection and dispersal assumes a fundamental role in the assessment of the volcanic hazards posed to the population living around the volcano or to the air traffic.

In spite of the large ash plume dispersed in the atmosphere, infrasound signals recorded during the explosive phases of March 2016 appear to be very weak, likely indicating low overpressures involved in the eruptive process. Assuming a simplified linear theory of sound, we estimate that the gas-ash mixture is ejected with velocities around 10–20 m/s, which are consistent with the immediate bending of the plume observed during the explosive phases.

Characterizing the main features of the ash fragments helps in discriminating the eruptive dynamics and fragmentation processes associated with periods of ash emission activity. The large amount of dispersed ash is interpreted as the result of the rigid fragmentation of an ascending and degassing magmatic column at low overpressure under impulsive, high-frequency explosive activity. Infrasound recordings demonstrate that this process is driven at Copahue by a low decompression rate compared to magmatic explosions typical of classical Strombolian activity. The low decompression rates may be related to the passage of the erupting mixture through an ash-filled crater and by the incorporation of recycled ash into the mixture. The recognition of the presence of a large amount of thermally modified, recycled material in the erupted products has important consequences for the interpretation of the general dynamics of the eruption. In terms of fragmentation and the energy needed for fragmentation, REC fragments can be considered as lithic material. Nevertheless, due to their high temperature at time of eruption, REC fragments also played an important role in releasing heat to the plume, hence contributing to the enhancement of convective power and dispersal of the ash. We suggest that the identification of such material can be crucial to understand the effective hazard potential of ash dispersal. This is particularly important for eruptions with unsteady dynamics, including weak ash emissions and violent Strombolian or Vulcanian explosions, resulting in pulsating and prolonged eruptive activity.

Acoustic records generated by Copahue activity are fully compatible in frequency as well as in amplitude to the acoustic signals generated by strombolian activity of Villarrica volcano and recorded at 193 km distance from the array. This similarity supports our conclusion that ash emission activity at Copahue is driven by low-pressure dynamics which is almost one order of magnitude weaker than that recorded for Villarrica. In spite of the weak infrasonic signals, which are commonly hidden by the noise generated by the strong eastward-directed winds, we also show how the infrasonic array is able to retrieve coherent detections which could be used to notify the onset of these low-pressure explosive dynamics.

In the past 20 years, infrasound has significantly increased the potential of volcano monitoring (e.g. Le Pichon et al., 2005; Dabrowa et al., 2011; Matoza et al., 2011), and it can be used to deliver early warnings of explosive eruptions (Garces et al., 2004; Ripepe and Marchetti, 2018). Here we have shown how infrasound is efficient at detecting volcanic activity in very windy environment also at regional distances. The results presented in our work support this strategy of monitoring volcanoes at regional scales (Dabrowsa et al., 2011; Matoza et al., 2011; Marchetti et al., 2019), and our results represent a starting point to establish an infrasonic network of multiple arrays on the eastern side of the Southern Andes.

DATA AVAILABILITY STATEMENT

The raw data supporting the conclusions of this article will be made available by the authors, without undue reservation.

AUTHOR CONTRIBUTIONS

MH, MR, GL, VM, RC wrote the manuscript. MH, MR, GL, VM, AC, have installed and processed the infrasonic array at Copahue. OV contributed with seismic and volcano logical observations. C-F provided the atmospheric profile and part of ray propagation. PG and RC have analyzed the ash samples.

FUNDING

The work was partially supported by the EUROVOLC (https://eurovolc.eu) funded by the European Community's Horizon 2020 program (grant agreement 731070).

ACKNOWLEDGMENTS

The authors wish to thank to the Laboratorio Geofisica Sperimentale of Università degli Studi Firenze, Mr. Adrián Arias and Caviahue community for their help and support. The research has been funded by project PI 40-A-497 (UNRN) and by the EUROVOLC (https://eurovolc.eu) funded by the European Community's Horizon 2020 program (grant agreement 731070). We greatly appreciated valuable revisions from three anonymous reviewers and associate editor John Stix.

SUPPLEMENTARY MATERIAL

The Supplementary Material for this article can be found online at: https://www.frontiersin.org/articles/10.3389/feart.2021.578437/full#supplementary-material.

REFERENCES

Agusto, M. R., and Vélez, M. L. (2017). Avances en el conocimiento del sistema volcánico-hidrotermal del Cpopahue: a 100 años del trabajo pionero de Don Pablo groeber. *Revista de la Asociacion Geologica Argentina*. 74 (1), 109–124.

Agusto, M. R., Caselli, A., Daga, R., Varekamp, J., Trinelli, A., Afonso, M. D. S., et al. (2017). *The crater lake of Copahue volcano (Argentina): geochemical and thermal changes between 1995 and 2015*. London, Geological SocietySpecial Publications, 437. 107–130. doi:10.1144/SP437.16

Andronico, D., and Cioni, R. (2002). Contrasting styles of mount vesuvius activity in the period between the avellino and pompeii plinian eruptions, and some implications for assessment of future hazards. *Bull. Volcanol* 64 (6), 372–391. doi:10.1007/s00445-002-0215-4

Battaglia, J., Hidalgo, S., Bernard, B., Steele, A., Arellano, S., and Acuña, K. (2019). Autopsy of an eruptive phase of Tungurahua volcano (Ecuador) through coupling of seismo-acoustic and SO2 recordings with ash characteristics. *Earth Planet. Sci. Lett.*, 511, 223–232. doi:10.1016/j.epsl.2019.01.042

Bonadonna, C., Genco, R., Gouhier, M., Pistolesi, M., Cioni, R., Alfano, F., et al. (2011). Tephra sedimentation during the 2010 Eyjafjallajökull eruption (Iceland) from deposit, radar, and satellite observations. *J. Geophys. Res. Solid Earth*, 116 (B12). doi:10.1029/2011JB008462

Bonadonna, C., Folch, A., Loughlin, S., and Puempel, H. (2012). Future developments in modelling and monitoring of volcanic ash clouds: outcomes from the first IAVCEI-WMO workshop on Ash dispersal forecast and Civil aviation. *Bull. Volcanol* 74, 1–10. doi:10.1007/s00445-011-0508-6

Bonali, F. L., Corazzato, C., Bellotti, F., and Groppelli, G. (2016). "Active tectonics and its interactions with Copahue volcano," in *Copahue volcano* (Berlin, Heidelberg), 23–45.

Caselli, A. T., Agusto, M., Velez, M. L., Forte, P., Bengoa, C., Daga, R., et al. (2016a). The 2012 eruptionTassiCopahue Volcano. in *Active volcanoes of the world. Book Series*. Editors F. En and O. Vaselliy (Heidelberg: Springer-Verlag), 61–77.

Caselli, A. T., Liccioli, C., and Tassi, F. (2016b). Risk assessment and mitigation at Copahue volcano. in *Copahue volcano* (Berlin, Heidelberg: Springer), 239–254. doi:10.1007/978-3-662-48005-2_10

Caselli, A. T., Sommer, C., and Barion, G. (2017a). *Conos piroclásticos anidados en el crater del volcán CopahueAgentina*, Argentina: Actas del XX Congreso Geológico Argentino, San Miguel de Tucmuna, 27-29. 24–26.

Caselli, A. T., Sommer, C., Daga, R., Baez, A., Albite, J., and Barion, G. (2017b). Caracterización de las fases eruptivas del volcán Copahue durante el ciclo 2012-2017 (Andes argentino-chileno). *Actas del XX Congreso Geológico ArgentinoSan Miguel de Tucmuna, Tucuman*, (Argentina: Springer), 27–29.

Cashman, K. V., and Scheu, B. (2015). Magmatic fragmentation. *The encyclopedia of volcanoes*. Academic Press, 459–471.

Cioni, R., Pistolesi, M., Bertagnini, A., Bonadonna, C., Hoskuldsson, A., and Scateni, B. (2014). Insights into the dynamics and evolution of the 2010 Eyjafjallajökull summit eruption (Iceland) provided by volcanic ash textures. *Earth Planet. Sci. Lett.* 394, 111–123. doi:10.1016/j.epsl.2014.02.051

Cocco, R., Karri, S. R., and Knowlton, T. (2014). Introduction to fluidization. *Chem. Eng. Prog.* 110 (11), 21–29.

D'Oriano, C., Pompilio, M., Bertagnini, A., Cioni, R., and Pichavant, M. (2012). Effects of experimental reheating of natural basaltic ash at different temperatures and redox conditions. *Contrib. Mineral. Petrol.* 165, 863–883. doi:10.1007/s00410-012-0839-0

D'Oriano, C., Bertagnini, A., Cioni, R., and Pompilio, M. (2014). Identifying recycled ash in basaltic eruptions. *Sci. Rep.* 4, 5851. doi:10.1038/srep05851

Dabrowa, A. L., Green, D. N., Rust, A. C., and Phillips, J. C. (2011). A global study of volcanic infrasound characteristics and the potential for long-range monitoring. *Earth Planet. Sci. Lett.* 310, 369–379. doi:10.1016/j.epsl.2011.08.027

Daga, R., Caselli, A., Ribeiro Guevara, S., and Agusto, M. (2017). Tefras emitidas durante la fase inicial hidromagmática (Julio de 2012) del ciclo eruptivo 2012 – actual (2016) del Volcán Copahue (ander del Sur). *Revista de la Asociación Geológica Argentina* 74, 191–206.

De Angelis, S., Lamb, O. D., Lamur, A., Hornby, A. J., von Aulock, F. W., Chigna, G., et al. (2016). Characterization of moderate ash-and-gas explosions at Santiaguito volcano, Guatemala, from infrasound waveform inversion and thermal infrared measurements. *Geophys. Res. Lett.* 43, 6220–6227. doi:10.1002/2016GL069098

de Groot-Hedlin, C., Hedlin, M. A., Walker, K. T., Drob, D., and Zumberge, M. A. (2008). Evaluation of infrasound signals from the shuttle Atlantis using a large seismic network. *J. Acoust. Soc. Am.* 124, 1442–1451. doi:10.1121/1.2956475

Deardorff, N., and Cashman, K. (2017). Rapid crystallization during recycling of basaltic andesite tephra: timescales determined by reheating experiments. *Sci. Rep.* 7, 46364. doi:10.1038/srep46364

Delle Donne, D., Ripepe, M., Lacanna, G., Tamburello, G., Bitetto, M., and Aiuppa, A. (2016). Gas mass derived by infrasound and UV cameras: implications for mass flow rate. *J. Volcanology Geothermal Res.* 325, 169–178. doi:10.1016/j.jvolgeores.2016.06.015

Dellino, P., Gudmundsson, M. T., Larsen, G., Mele, D., Stevenson, J. A., Thordarson, T., et al. (2012). Ash from the Eyjafjallajökull eruption (Iceland): fragmentation processes and aerodynamic behavior. *J. Geophys. Res. Solid Earth* 117 (B9). doi:10.1029/2011jb008726

D'Oriano, C., Cioni, R., Bertagnini, A., Andronico, D., and Cole, P. D. (2011). Dynamics of ash-dominated eruptions at Vesuvius: the post-512 AD AS1a event. *Bull. Volcanol* 73, 699–715. doi:10.1007/s00445-010-0432-1

Fee, D., and Matoza, R. S. (2013). An overview of volcano infrasound: from Hawaiian to plinian, local to global. *J. Volcanology Geothermal Res.* 249, 123–139. doi:10.1016/j.jvolgeores.2012.09.002

Fee, D., Izbekov, P., Kim, K., Yokoo, A., Lopez, T., Prata, F., et al. (2017). Eruption mass estimation using infrasound waveform inversion and ash and gas measurements: evaluation at Sakurajima Volcano, Japan. *Earth Planet. Sci. Lett.* 480, 42–52. doi:10.1016/j.epsl.2017.09.043

Folguera, A., Vera, E. R., Vélez, L., Tobal, J., Orts, D., Agusto, M., et al. (2016). "*A review of the geology, structural controls, and tectonic setting of Copahue volcano, Southern Volcanic Zone, Andes, Argentina*", "in *Copahue volcano*. Editor F. Tassi, O. y. Vaselli, and A. Caselli, Springer, Berlin, Heidelberg. 3–22. doi:10.1007/978-3-662-48005-2_1

Garcés, M., Fee, D., Steffke, A., McCormack, D., Servranckx, R., Bass, H., et al. (2008). Capturing the acoustic fingerprint of stratospheric ash injection. *Eos Trans. AGU* 89 (40), 377–378. doi:10.1029/2008eo400001

Garcés, M., Willis, M., Hetzer, C., Pichon, A. L., and Drob, D. (2004). On using ocean swells for continuous infrasonic measurements of winds and temperature in the lower, middle, and upper atmosphere. *Geophys. Res. Lett.* 31, L19304. doi:10.1029/2004GL020696

Gaunt, H. E., Bernard, B., Hidalgo, S., Proaño, A., Wright, H., Mothes, P., et al. (2016). Juvenile magma recognition and eruptive dynamics inferred from the analysis of ash time series: the 2015 reawakening of Cotopaxi volcano. *J. Volcanology Geothermal Res.* 328, 134–146. doi:10.1016/j.jvolgeores.2016.10.013

Global Volcanism Program.(2013). Report on Copahue (Chile-Argentina)," *Bulletin of the global volcanism network*. florence italy. Editors J. A. Herrick and R. Wunderman (Smithsonian Institution), 38 (9). doi:10.5479/si.GVP.BGVN201309-357090

Global Volcanism Program (2016). Report on Copahue (Chile-Argentina). *Bulletin of the global volcanism network*. florence italy. Editor E. Venzke (Smithsonian Institution), 41, 3. doi:10.5479/si.GVP.BGVN201603-357090

Goto, A., and Johnson, J. B. (2011). Monotonic infrasound and helmholtz resonance at volcan Villarrica (Chile). *Geophys. Res. Lett.* 38, a. doi:10.1029/2011GL046858

Gudmundsson, M. T., Thordarson, T., Höskuldsson, Á., Larsen, G., Björnsson, H., Prata, F. J., et al. (2012). "Ash generation and distribution from the April-May 2010 eruption of Eyjafjallajökull", *Iceland. Scientific Reports*. 2, 1–12.

Houghton, B. F., and Nairn, I. A. (1991). The 1976?1982 Strombolian and phreatomagmatic eruptions of White Island, New Zealand: eruptive and depositional mechanisms at a ?wet? volcano. *Bull. Volcanol* 54 (1), 25–49. doi:10.1007/bf00278204

Houghton, B. F., and Smith, R. T. (1993). Recycling of magmatic clasts during explosive eruptions: estimating the true juvenile content of phreatomagmatic volcanic deposits. *Bull. Volcanol* 55, 414–420. doi:10.1007/bf00302001

Johnson, J. B., and Ripepe, M. (2011). Volcano infrasound: a review. *J. Volcanology Geothermal Res.* 206, 61–69. doi:10.1016/j.jvolgeores.2011.06.006

Johnson, J. B. (2003). Generation and propagation of infrasonic airwaves from volcanic explosions. *J. Volcanology Geothermal Res.* 121, 1–14. doi:10.1016/S0377-0273(02)00408-0

Kim, K., Fee, D., Yokoo, A., and Lees, J. M. (2015). Acoustic source inversion to estimate volume flux from volcanic explosions. *Geophys. Res. Lett.* 42, 5243–5249. doi:10.1002/2015GL064466

Kremers, S., Scheu, B., Cordonnier, B., Spieler, O., and Dingwell, D. B. (2010). Influence of decompression rate on fragmentation processes: an experimental study. *J. Volcanology Geothermal Res.* 193, 182–188. doi:10.1016/j.jvolgeores.2010.01.015

Kueppers, U., Scheu, B., Spieler, O., and Dingwell, D. B. (2006). Fragmentation efficiency of explosive volcanic eruptions: a study of experimentally generated pyroclasts. *J. Volcanology Geothermal Res.* 153 (1-2), 125–135. doi:10.1016/j.jvolgeores.2005.08.006

Lacanna, G., and Ripepe, M. (2013). Influence of near-source volcano topography on the acoustic wavefield and implication for source modeling. *J. Volcanology Geothermal Res.* 250, 9–18. doi:10.1016/j.jvolgeores.2012.10.005

Lacanna, G., and Ripepe, M. (2020). Modelling the acoustic flux inside the magmatic conduit by 3D-FDTD simulation. *J. Geophys. Res. Solid Earth*. doi:10.1029/2019JB018849

Lacanna, G., Ichihara, M., Iwakuni, M., Takeo, M., Iguchi, M., and Ripepe, M. (2014). Influence of atmospheric structure and topography on infrasonic wave propagation. *J. Geophys. Res. Solid Earth* 119 (4), 2988–3005. doi:10.1002/2013JB010827

Le Pichon, A., Blanc, E., Drob, D., Lambotte, S., Dessa, J. X., Lardy, M., et al. (2005). Infrasound monitoring of volcanoes to probe high-altitude winds. *J. Geophys. Res.* 110, D13106,. doi:10.1029/2004JD005587

Linares, E., Ostera, H. A., and Mas, L. (1999). Cronología Potasio-Argón del complejo efusivo Copahue–Caviahue, Provincia de Neuquén. *Revista de la Asociación Geológica Argentina* 54 (3), 240–247.

Maekawa, Z. (1968). Noise reduction by screens. *Appl. Acoust.* 1, 157–173. doi:10.1016/0003-682x(68)90020-0

Marchetti, E., Ripepe, M., Campus, P., Le Pichon, A., Vergoz, J., Lacanna, G., et al. (2019). Long range infrasound monitoring of Etna volcano. *Scientific Rep.* 9 (1), 18015, doi:10.1038/s41598-019-54468-5

Martini, M., Bermúdez, A., Delfino, D., and Giannini, L. (1997). *The thermal manifestations of Copahue Volcano area. Neuquén*. Argentina, VIII Congreso Geológico Chileno Antofagasta, 4, 352–356.

Matoza, R. S., Le Pichon, A., Vergoz, J., Herry, P., Lalande, J.-M., Lee, H.-i., et al. (2011). Infrasonic observations of the June 2009 Sarychev Peak eruption, Kuril Islands: implications for infrasonic monitoring of remote explosive volcanism. *J. Volcanology Geothermal Res.* 200, 35–48. doi:10.1016/j.jvolgeores.2010.11.022

Rybin, D., Folguera, A., and Ramos, V. A. (2006). Structural control on arc volcanism: the Caviahue-Copahue complex, Central to Patagonian Andes transition (38°S). *J. South Am. Earth Sci.* 22, 66–88. doi:10.1016/j.jsames.2006.08.008

Miwa, T., Toramaru, A., and Iguchi, M. (2009). Correlations of volcanic ash texture with explosion earthquakes from Vulcanian eruptions at Sakurajima volcano, Japan. *J. Volcanology Geothermal Res.* 184 (3-4), 473–486. doi:10.1016/j.jvolgeores.2009.05.012

Naranjo, J. A., and Polanco, E. (2004). The 2000 AD eruption of Copahue volcano, southern Andes. *Revista Geológica de Chile* 31 (2), 279–292. doi:10.4067/s0716-02082004000200007

Ono, K., Watanabe, K., Hoshizumi, H., and Ikebe, S. I. (1995). Ash eruption of the Naka-dake crater, Aso volcano, southwestern Japan. *J. volcanology geothermal Res.* 66 (1-4), 137–148. doi:10.1016/0377-0273(94)00061-k

OVDAS-SERNAGEOMIN (2016a). *Reporte de Actividad volcanica (RAV), region de laAraucanía, abril – volumen 04*. Temuco: Servicio Nacional de Geologia y Mineria.

OVDAS-SERNAGEOMIN (2016b). *Reporte de Actividad Volcanica (RAV), Region del Biobío, marzo – volumen 06*. Temuco: Servicio Nacional de Geologia y Mineria.

Petrinovic, I. A., Villarosa, G., D´Elia, L., Guzmán, S. P., Páez, G. N., Outes, V., et al. (2014). *La erupción del 22 de diciembre de 2012 del volcán Copahue Neuquén*. Argentina. Revista de la Asociación Geológica Argentina, caracterización del ciclo eruptivo y sus productos, 71 (2), 161–173.

Ripepe, M., and Marchetti, E. (2002). Array tracking of infrasonic sources at Stromboli volcano. *Geophys. Res. Lett.* 29 (22), 33. doi:10.1029/2002GL015452

Ripepe, M., and Marchetti, E. (2018). *Infrasound Monitoring of volcanic-related hazard for civil protection*. in *Infrasound monitoring for atmospheric studies: challenge in middle-atmosphere dynamics and societal benefits*. Editors A. Le Pichon, E. Blanc, and A. Hauchecomepp. 2 Edn (Springer). doi:10.1007/978-3-319-75140-5

Ripepe, M., Marchetti, E., and Ulivieri, G. (2007). Infrasonic monitoring at Stromboli volcano during the 2003 effusive eruption: insights on the explosive and degassing process of an open conduit system. *J. Geophys. Res.* 112. doi:10.1029/2006JB004613

Ripepe, M., Marchetti, E., Bonadonna, C., Harris, A. J. L., Pioli, L., and Ulivieri, G. (2010). Monochromatic infrasonic tremor driven by persistent degassing and convection at Villarrica Volcano, Chile. *Geophys. Res. Lett.* 37, doi:10.1029/2010GL043516

Ripepe, M., Bonadonna, C., Folch, A., Delle Donne, D., Lacanna, G., Marchetti, E., et al. (2013). Ash-plume dynamics and eruption source parameters by infrasound and thermal imagery: the 2010 Eyjafjallajökull eruption. *Earth Planet. Sci. Lett.* 366, 112–121. doi:10.1016/j.epsl.2013.02.005

Ripepe, M., Marchetti, E., Delle Donne, D., Genco, R., Innocenti, L., Lacanna, G., et al. (2018). Infrasonic early warning system for explosive eruptions. *J. Geophys. Res. Solid Earth* 123, 9570. doi:10.1029/2018JB015561

Spieler, O., Kennedy, B., Kueppers, U., Dingwell, D. B., Scheu, B., and Taddeucci, J. (2004). The fragmentation threshold of pyroclastic rocks. *Earth Planet. Sci. Lett.* 226 (1-2), 139–148. doi:10.1016/j.epsl.2004.07.016

Ulivieri, G., Ripepe, M., and Marchetti, E. (2013). Infrasound reveals transition to oscillatory discharge regime during lava fountaining: implication for early warning. *Geophys. Res. Lett.* 40 (12), 3008–3013. doi:10.1002/grl.50592

Wohletz, K., Zimanowski, B., and Büttner, R. (2013). *Magma-water interactions. Modeling volcanic processes*. New York: Cambridge University Press, 230–257.

Woods, A. W., and Bower, S. M. (1995). The decompression of volcanic jets in a crater during explosive volcanic eruptions. *Earth Planet. Sci. Lett.* 131 (3-4), 189–205. doi:10.1016/0012-821x(95)00012-2

Conflict of Interest: The authors declare that the research was conducted in the absence of any commercial or financial relationships that could be construed as a potential conflict of interest.